



Design and Stress Analysis of FRP Composite Pressure Vessel

M.A. Mujeeb Iqbal¹ | Mohd.Hasham Ali² | Mohammed Fareed³

¹Assistant Professor, Department of Mechanical Engineering, Muffakham Jah College of Engineering & Technology, Hyderabad, Telanagana, India.

²Assistant Professor, Department of Mechanical Engineering, Muffakham Jah College of Engineering & Technology, Hyderabad, Telanagana, India.

³Assistant Professor, Department of Mechanical Engineering, Vidya Jyothi Institute of Technology, Aziz Nagar, Hyderabad, Telanagana, India.

ABSTRACT

Pressure vessels are containers that operate at pressures above atmospheric pressure. A pressure vessel can be defined as a relatively high-volume pressure component (such as a spherical or cylindrical container) that has a cross section larger than the associated pipe or tubing. The composite materials have been widely used for the manufacturing of pressure vessels from a very long time. These pressure vessels are manufactured by filament winding process. The filament wound composite pressure vessels have special characteristics of high strength to modulus ratio. The Filament wound composite pressure vessels have become very popular in various industries and applications that include aerospace, sewage, chemical, oil and gas industries. During operation these pressure vessels are subjected to very high internal pressures and very high internal stresses are developed in them. The safety aspect is vital because of high working pressure and build-up of high stresses in the pressure vessel. Therefore the stress and burst pressure analysis are essential for the safe working and performance evaluation of such pressure vessels.

Finite element model of the multilayered filament wound composite pressure vessel is established by the finite element software ANSYS 12. The pressure vessel is analyzed for maximum stress and its burst pressure is predicted for hoop and helical windings of the fibers using a failure model such as the Tsai-Wu failure criterion. The fibers are oriented helically for various orientations such as (+30/-30)s, (+35,-35)s, (+40,-40)s, (+45/-45)s, (+50,-50), (+55/-55)s, (+60,-60) and (+65/-65)s. Based on the maximum stress criteria, burst pressure and optimum angle of fiber orientation were determined from the analysis. The aim of this paper is to analyze stresses in a Glass filament wound FRP pressure vessel for different winding orientations using Ansys 12, and compute the burst pressure of the vessel by applying a suitable failure criterion. This paper aims at developing composite pressure vessel using E-Glass, and this work will be extremely useful for FRP-equipment manufacturers, designers, and consultants in the field of chemical process industries.

KEYWORDS: Composite pressure vessels, filament winding, finite element analysis, internal pressure, boundary conditions, fiber orientations

Copyright © 2015 International Journal for Modern Trends in Science and Technology
All rights reserved.

I. INTRODUCTION

Pressure vessels have been manufactured by filament winding for a long time. Although they appear to be simple structures, pressure vessels are among the most difficult to design. Filament-wound composite pressure vessels have found widespread use not only for military use but also for civilian applications. This technology originally developed for the military's internal use was adapted to civilian purpose and later extended to the commercial market. Applications include breathing device, such as

self-contained breathing apparatuses used by fire-fighters and other emergency personnel, scuba tanks for divers, oxygen cylinders for medical and aviation cylinders for emergency slide inflation, opening doors or lowering of landing gear, mountaineering expedition equipment, paintball gas cylinders, etc. A potential widespread application for composite pressure vessels is the automotive industry. Emphasis on reducing emissions promotes the conversion to Compressed Natural Gas (CNG) fuelled vehicles worldwide. Engineers are seeking to replace fuel oils with natural gas or hydrogen as the energy supply in automobiles for air quality improvements and

reduce global warming. Fuel cells in concert with hydrogen gas storage technologies are key requirements for the successful application of these fuels in vehicles. One of the limitations is lack of vehicle range between refuelling stops. Weight, volume and cost of the containment vessel are also considerations.

II. FINITE ELEMENT ANALYSIS

2.1 Introduction to FE Analysis

Finite element analysis is a powerful numerical technique for analysis. FEA is used for stress analysis in that area of solid mechanics. The basic concept of finite element method is that a body / structure may be divided into smaller elements called finite elements. The properties of the element are formulated and combined to obtain the solution for the entire body or structure. For a given practical design problem the engineer has to idealize the physical system into a FE model with proper boundary conditions and loads that are acting on the system. Then the discretization of a given body or structure into cells of finite elements is performed and the mathematical model is analyzed for every element and then for complete structure. The various unknown parameters are computed by using known parameters.

2.1.1 Steps involved in ANSYS Preprocessor :

Preprocessor Inputs are

- (1) Element type
- (2) Real constants
- (3) Material properties (young's modulus, Poisons ratio, shear modulus)
- (4) Meshing

Boundary conditions :

The boundary conditions like displacement and pressure are applied.

Solution:

General post processor:

In the General post processor the results obtain are deformation mechanical, and Stress

2.2 General Element Features

2.2.1 Element Input

2.2.1.1 Element Name

2.2.1.2 Nodes

2.2.1.3 Degrees of Freedom

2.2.1.4 Real Constants

2.2.1.5 Material properties

2.2.1.6 Surface Loads

2.2.1.1 Element Name : An element type is identified by a name (8 characters maximum), such as PLANE82 consisting of a group label (PLANE) and a unique, identifying number (82). The element descriptions in *Element Library* are arranged in order of these identification numbers. The element is selected from the library for use in the analysis by inputting its name on the element type command

2.2.1.2 Nodes: The nodes associated with the element are listed as I, J, K, etc. Elements are connected to the nodes in the sequence and orientation shown on the input figure for each element type. This connectivity can be defined by automatic meshing, or may be input directly by the user with the **E** command.

2.2.1.3 Degrees of Freedom: Each element type has a degree of freedom set, which constitute the primary nodal unknowns to be determined by the analysis. They may be displacements, rotations, temperatures, pressures, voltages, etc. Derived results, such as stresses, heat flows, etc., are computed from these degree of freedom results. Degrees of freedom are not defined on the nodes explicitly by the user, but rather are implied by the element types attached to them. The choice of element types is therefore, an important one in any ANSYS analysis.

2.2.1.4 Real Constants: Data which are required for the calculation of the element matrix, but which cannot be determined from the node locations or material properties, are input as "real constants." Typical real constants include area, thickness, inner diameter, outer diameter, etc.

2.2.1.5 Material properties: Various material properties are used for each element type. Typical material properties include Young's modulus (of elasticity), density, coefficient of thermal expansion, thermal conductivity, etc. Each property is referenced by an ANSYS label - EX, EY, and EZ for the directional components of Young's modulus, DENS for density, and so on. All material properties can be input as functions of temperature.

2.2.1.6 Surface Loads: Various element types allow surface loads. Surface loads are typically pressures for structural element types, convections or heat fluxes for thermal element types, etc.

2.3 Element type selection: Element : Structural Solid Quad 8 node 82 (Plane 82)

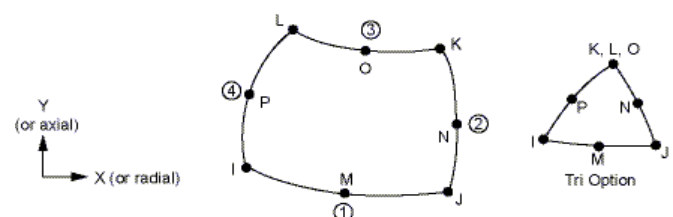


Figure 2.1 Plane82 Geometry

2.3.1 PLANE82 Element Description: PLANE82 is a higher order version of the 2-D, four-node element. It provides more accurate results for mixed

(quadrilateral-triangular) automatic meshes and can tolerate irregular shapes without as much loss of accuracy. The 8-node elements have compatible displacement shapes and are well suited to model curved boundaries. The 8-node element is defined by eight nodes having two degrees of freedom at each node: translations in the nodal x and y directions. The element may be used as a plane element or as an axisymmetric element. The element has plasticity, creep, swelling, stress stiffening, large deflection, and large strain capabilities.

2.3.2 PLANE82 Input Summary

Nodes

I, J, K, L, M, N, O, P

Degrees of Freedom

UX, UY

Material Properties

EX, EY, EZ, PRXY, PRYZ, PRXZ (or NUXY, NUYZ, NUXZ),

Surface Loads

Pressures --

face 1 (J-I), face 2 (K-J), face 3 (I-K), face 4 (I-L)

2.3.3 Element Behaviour:

\Option K3 = Axisymmetry

2.3.4 Problem description:

The Glass fiber reinforced polymer composite pressure vessel is analyzed for two different cases

2.3.4.1 Case 1:

In the first case, the pressure vessel is subjected to working internal pressure of 35Mpa. The pressure vessel is analyzed for hoop and various helical fiber orientations (+30,-30)s, (+35,-35)s, (+40,-40)s, (+45,-45)s, (+50,-50)s, and (+55,-55)s for symmetrical stacking sequence.

2.3.4.2 Case 2:

In the second case the pressure vessel is subjected to high internal pressure values and the burst pressure of the pressure vessel is predicted for the same fiber orientations. The burst pressure for the pressure vessel is predicted by incrementally increasing the Values of internal pressure from a working pressure of 35Mpa.

2.4 Material properties of E-glass fiber reinforced polymer composite pressure vessel:

Table 2.1 Typical properties of filament wound pipes (glass fibre reinforced)

Property	Typical Values	Predominant Process Variables
Density	1.88-2.26	Glass/Resin Ratio
Tensile Strength, MPa (Helical Windings)	344-1034	Glass Type, Glass/Resin Ratio, Wind Pattern
Compressive Strength, MPa (Helical Windings)	276-551	Glass/Resin Ratio, Resin Type, Wind Pattern
Shear Strength, MPa: --Interlaminar --Cross	21-137 55-206	Resin Type, Wind Pattern, Glass/Resin Ratio, Resin Type
Modulus of Elasticity (Tension), GPa	21-41	Glass type, Wind Pattern
Modulus of Rigidity (Torsion), GPa	11-14	Wind Pattern
Flexural Strength	344-517	Wind Pattern, Glass/Resin Ratio

Table 2.2 Linear material properties of filament wound pressure vessel (glass fibre reinforced)

MP, Value	Value (Gpa)	Description
EX	29.0	Elastic modulus, Element X-direction
EY	5.3	Elastic modulus, Element Y-direction
EZ	5.3	Elastic modulus, Element Z-direction
PRXY	0.44	Major poisson's ratio, XY Plane
PRYZ	0.20	Major poisson's ratio, YZ Plane
PRXZ	0.44	Major poisson's ratio, XZ Plane
GXY	5.11	Shear modulus, XY Plane
GXZ	5.11	Shear modulus, XZ Plane

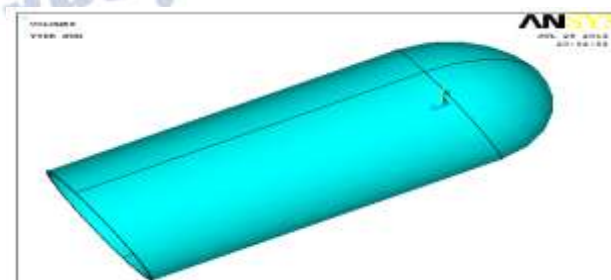


Fig 2.2 The above figure shows the finite element mode of the glass fiber reinforced composite pressure vessel

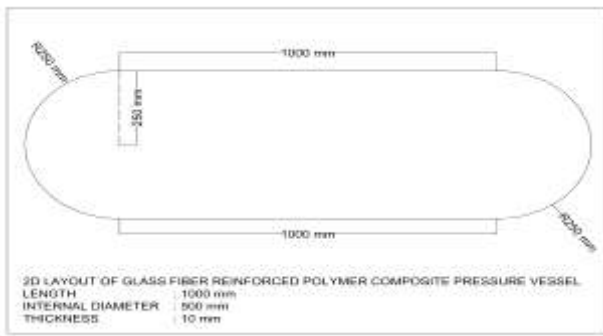


Figure 2.3 The above figure shows the geometric 2D-layout of GFRP composite pressure vessel

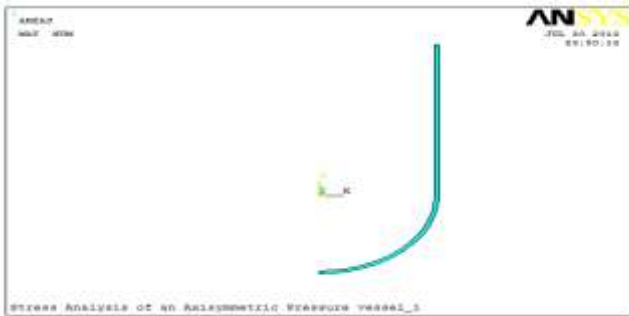


Figure 2.4 The above figure shows the axisymmetric model of GFRP composite pressure vessel

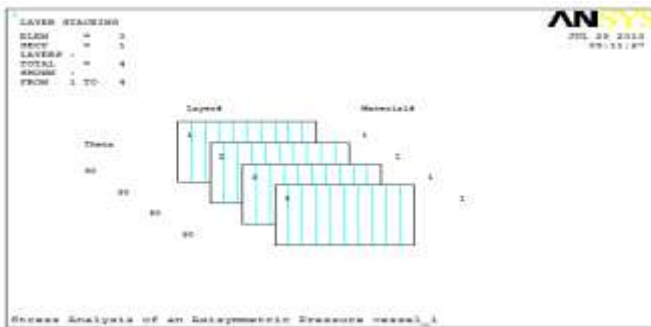


Figure 2.5 The above figure shows the stacking sequence for hoop direction (90 degrees) of fibers orientation angle of glass fiber reinforced composite pressure vessel

The above figure 2.5 shows the symmetrical stacking sequence for hoop direction for the Glass fiber reinforced composite vessel. Each layer thickness is equal to 2.5mm and four layers are selected for the analysis in symmetrical pattern with angle equal to 90 degrees fiber orientation.

2.5 Meshing:

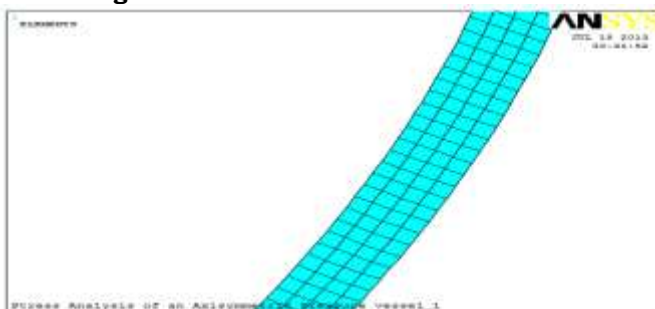


Figure: 2.6 The above figure shows a zoomed section of the meshed geometry of the Glass fiber reinforced composite pressure vessel along the thickness of the walls of the vessel.

The geometry of GFRP composite pressure is free meshed with Quad elements. All elements are approximately of same size and the element edge length is of 2.5mm.

2.6 Boundary conditions:

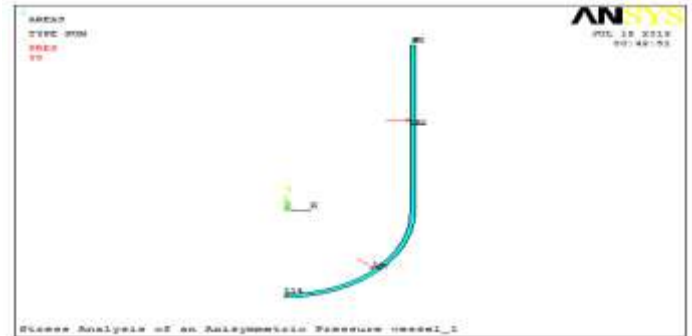


Figure 2.7 The above figure shows the boundary conditions applied to the GFRP composite pressure vessel and applied pressure of 35Mpa

The Boundary Conditions and Loads are now applied. ANSYS will automatically apply the Axisymmetric Boundary Conditions along the Y-axis. However, we must apply the Symmetry Boundary Conditions along the upper edge of the model. Finally, the Pressure equal to 35Mpa is applied on all lines that make up the inner surface of the vessel.

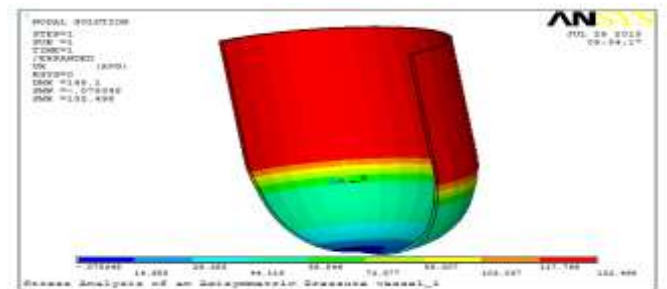


Figure 2.8 The above figure shows the maximum stress equal to 132.489, for the GFRP composite pressure vessel for hoop (90 degree fiber orientation angle) at working pressure of 35Mpa

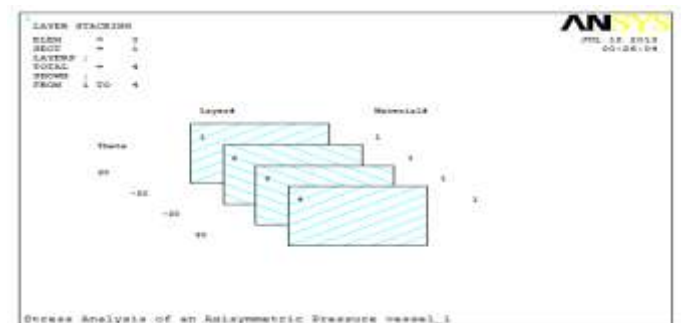


Figure 2.9 The above figure shows the stacking sequence of (+30,-30, -30, and +30) fiber orientation angles

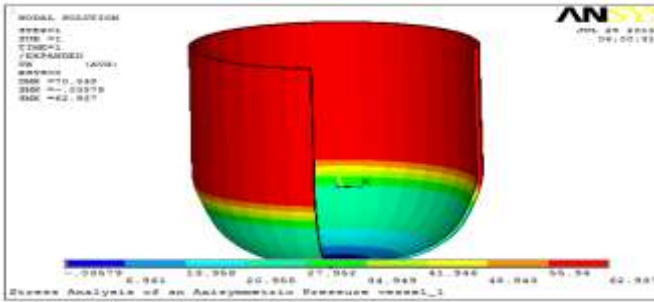


Figure 2.10 The above figure shows the maximum stress equal to 62.937Mpa, for the GFRP composite pressure vessel for (+30,-30, -30,and +30) fiber orientation angle at working pressure of 35Mpa

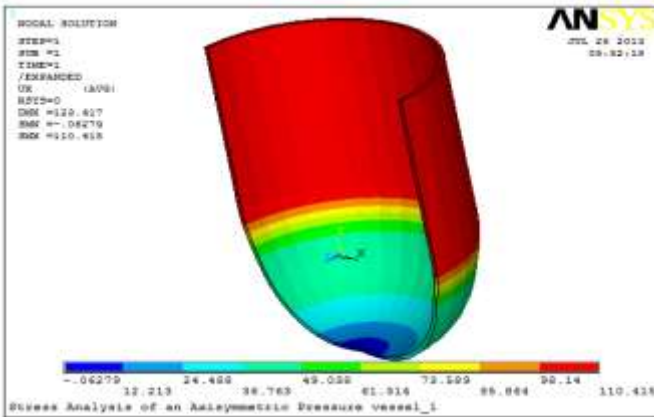


Figure 2.11 The above figure shows the burst pressure equal to 110.415Mpa, for the GFRP composite pressure vessel for (+30,-30, -30,and +30) fiber orientation angle

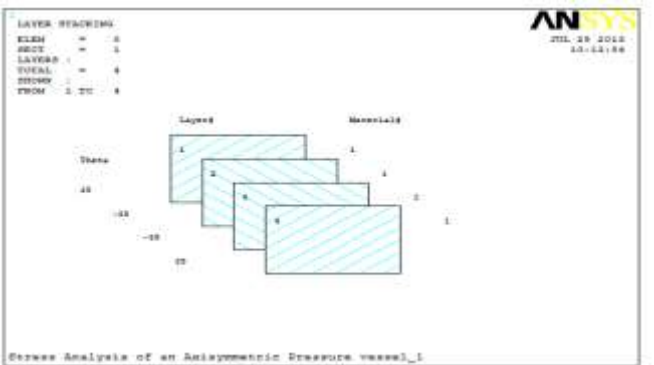


Figure 2.12 The figure shows the stacking sequence of (+35,-35, -35 ,and +35) fiber orientation angles

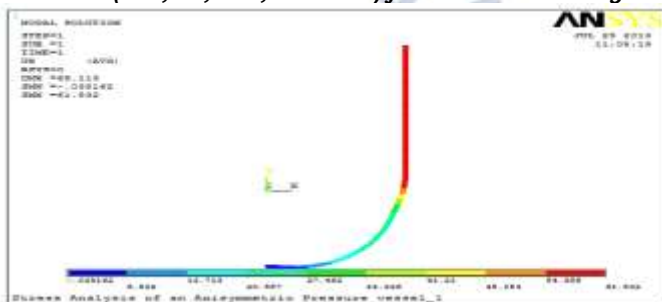


Figure 2.13 The above figure shows the maximum stress equal to 61.832Mpa, at working pressure of 35Mpa for (+35,-35, -35,and +35) fiber orientation angle

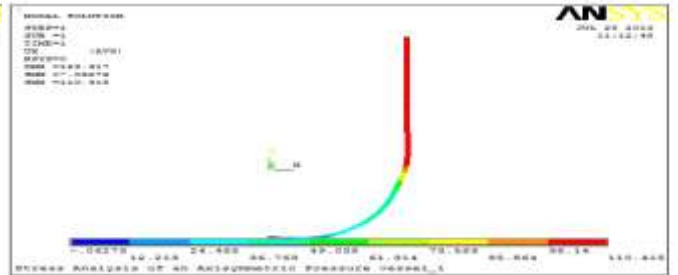


Figure 2.14 The above figure shows the burst pressure equal to 110.415Mpa, for the GFRP composite pressure vessel for (+35,-35, -35,and +35) fiber orientation angle

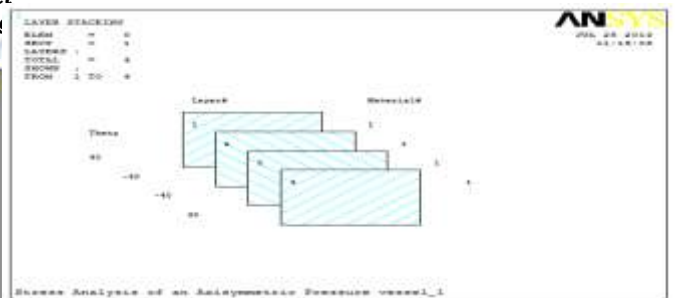


Figure 2.15 The figure shows the stacking sequence of (+40,-40, -40 ,and +40) fiber orientation angles

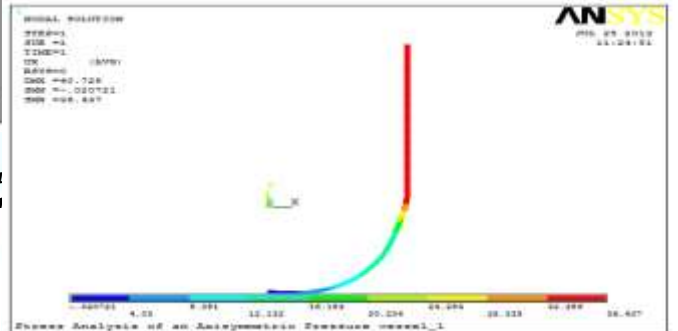


Figure 2.16 The above figure shows the maximum stress equal to 36.437Mpa, at pressure of 35Mpa for (+40,-40, -40 ,and +40) fiber orientation angle

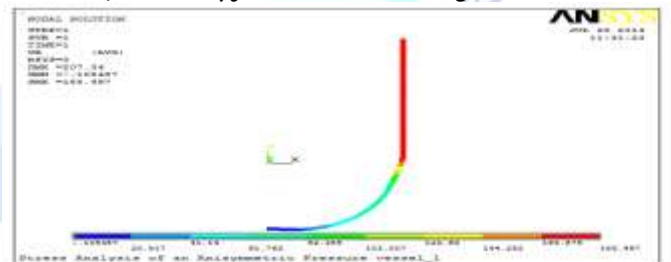


Figure 2.17 The above figure shows the burst pressure equal to 185.497Mpa, for the GFRP composite pressure vessel for (+40, -40, -40,and +40) fiber orientation

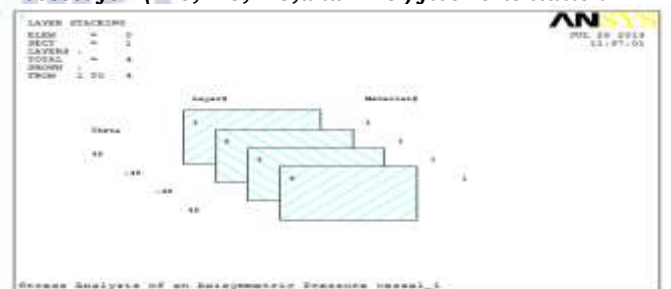


Figure 2.18 The figure shows the stacking sequence of (+45 ,-45, -45 ,and +45) fiber orientation angle

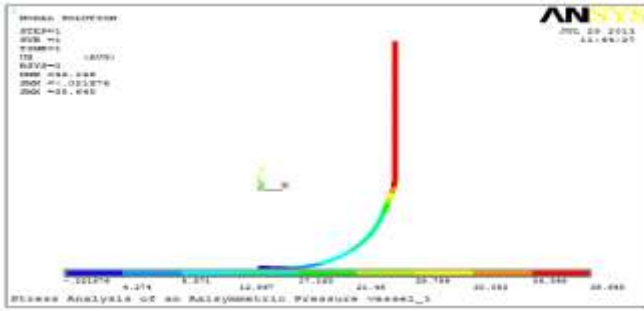


Figure 2.19 The above figure shows the maximum stress equal to 38.645Mpa, at pressure of 35Mpa for (+45, -45, -45,and +45) fiber orientation

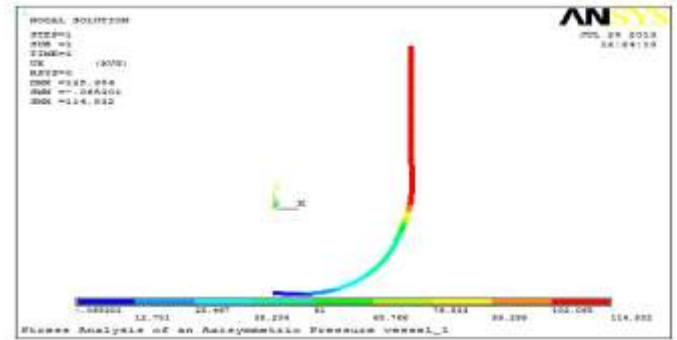


Figure 2.23 The above figure shows the burst pressure equal to 114.832Mpa , for the GFRP composite pressure vessel for (+50, -50, -50, and +50) fiber orientation angle

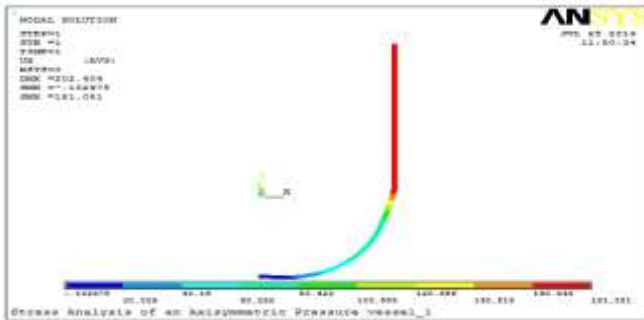


Figure 2.20 The above figure shows the burst pressure equal to 181.081Mpa , for the GFRP composite pressure vessel for (+45,-45, -45,and +45) fiber orientation angle

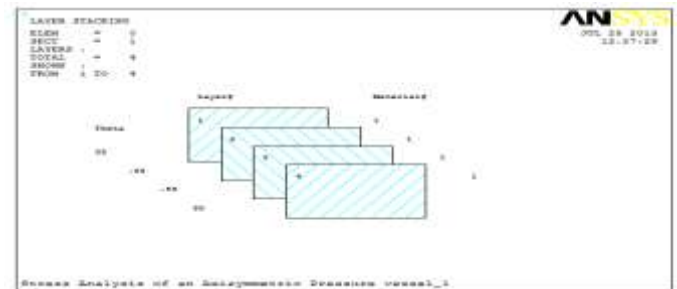


Figure 2.24 The figure shows the stacking sequence of (+55, -55, -55 ,and +55) fiber orientation angle

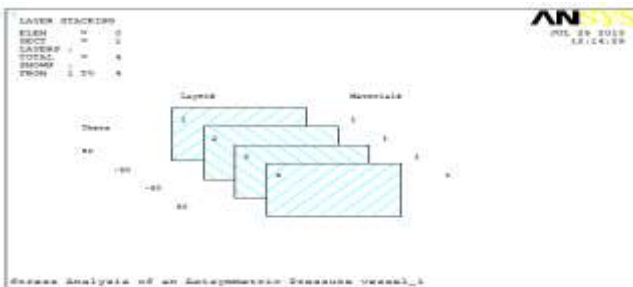


Figure 2.21 The figure shows the stacking sequence of (+50 , -50, -50 ,and +50) fiber orientation angle

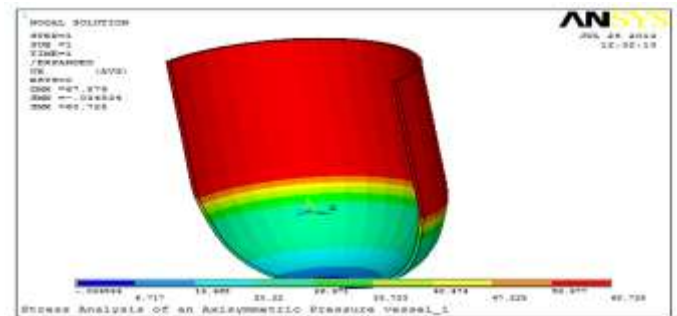


Figure 2.25 The above figure shows the maximum stress equal to 60.728Mpa, for the GFRP composite pressure vessel for (+55 ,-55 ,-55 ,and +55) fiber orientation angle at working pressure of 35Mpa

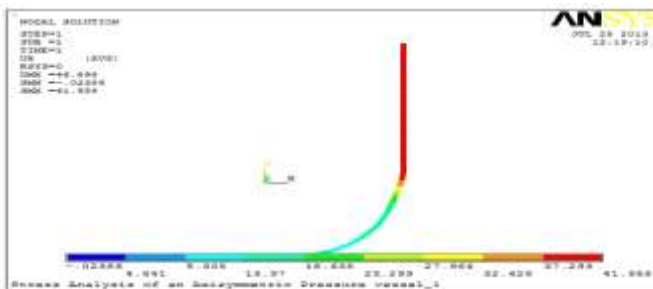


Figure 2.22 The above figure shows the maximum stress equal to 41.958Mpa, for the GFRP composite pressure vessel for (+50, -50 , -50 ,and +50) fiber orientation at working pressure of 35Mpa.

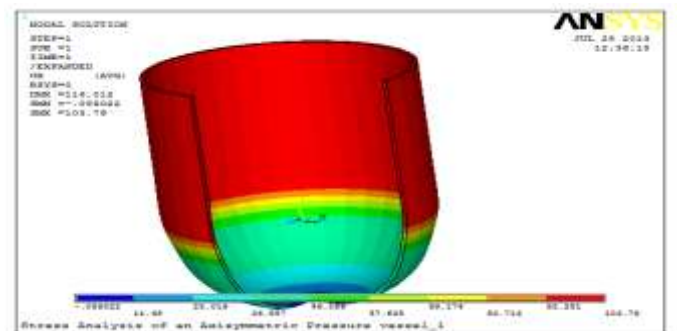


Figure 2.26 The above figure shows the burst pressure equal to 103.79, for the GFRP composite pressure vessel for (+55, -55, -55, and +55) fiber orientation angle

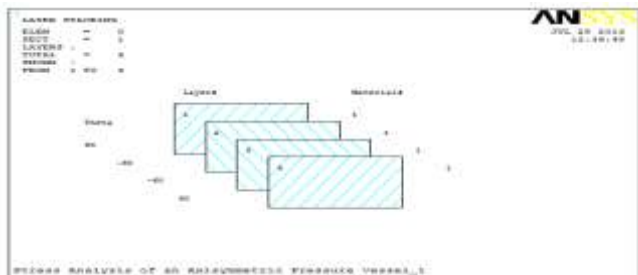


Figure 2.27 The above figure shows the stacking sequence of (+60, -60, -60, and +60) fiber orientation angle

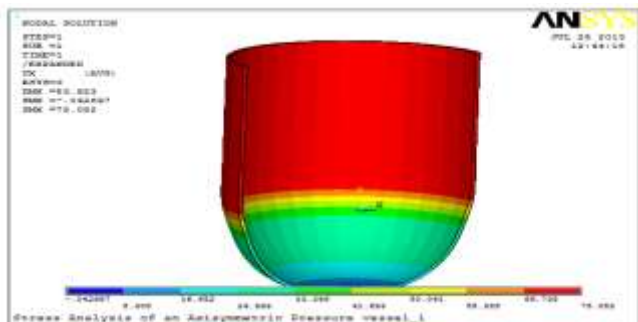


Figure 2.28 The above figure shows the maximum stress equal to 75.082Mpa, for the GFRP composite pressure vessel for (+60, -60, -60, and +60) fiber orientation angle at working pressure of 35Mpa

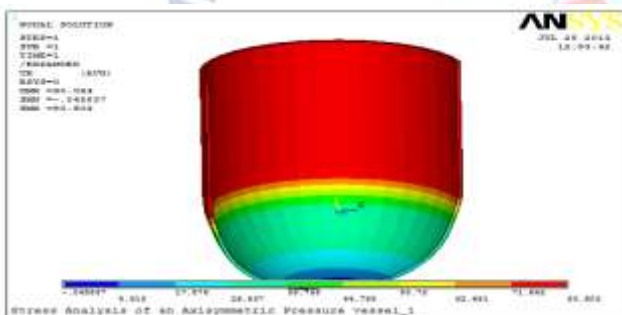


Figure 2.29 The above figure shows the burst pressure equal to 80.603Mpa, for the GFRP composite pressure vessel for (+60, -60, -60, and +60) fiber orientation angle

III. MATH

The results obtained after analysis are tabulated and shown below in table 3.1 and table 3.2

Table 3.1 shows the maximum stress for different fiber orientation angles

S. No	Angle of fiber orientation	Maximum stress (Mpa)
1	(+30, -30, -30, +30),symmetrical stacking	62.937
2	(+35, -35, -35, +35),symmetrical stacking	61.832
3	(+40, -40, -40, +40),symmetrical stacking	36.437
4	(+45, -45, -45, +45),symmetrical stacking	38.645
5	(+50, -50, -50, +50),symmetrical stacking	41.958
6	(+55, -55, -55, +55),symmetrical stacking	60.728
7	(+60, -60, -60, +60),symmetrical stacking	75.082

Table 3.2 shows the burst pressure for different fiber orientation angles

S. No	Angle of fiber orientation	Burst pressure (Mpa)
1	(+30, -30, -30, +30),symmetrical stacking	110.415
2	(+35, -35, -35, +35),symmetrical stacking	119.015
3	(+40, -40, -40, +40),symmetrical stacking	185.497
4	(+45, -45, -45, +45),symmetrical stacking	181.081
5	(+50, -50, -50, +50),symmetrical stacking	114.832
6	(+55, -55, -55, +55),symmetrical stacking	103.79
7	(+60, -60, -60, +60),symmetrical stacking	80.603

The results of the maximum stress analysis for various fiber orientations are plotted graphically and can be seen in form of below figure. The analysis of the stress distribution for the different fiber orientations shows that the maximum stress in the cylindrical composite pressure vessel is found to be minimum for (+40/-40)s fiber orientation.

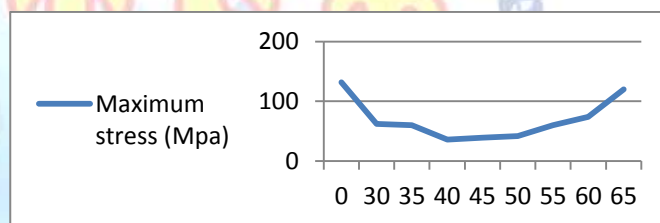


Figure: 3.1 Graph : variation of Maximum Stress (Mpa) with different fiber orientation angles

While, the results burst pressure analysis for various fiber orientations can be seen in the graph shown in figure below. The figure shows that the pressure vessel can bear maximum internal pressure of 186Mpa at (+40,-40,-40,+40) fiber orientation angle.

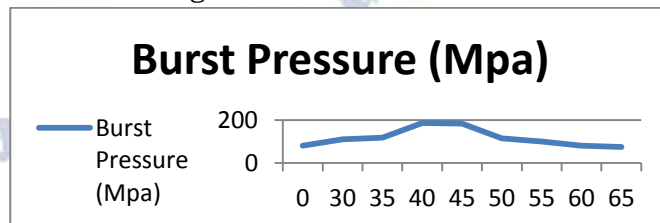


Figure:3.2 Graph :variation of burst pressure (Mpa) with different fiber orientation angles.

IV. CONCLUSION & FUTURE SCOPE

The analysis of the stress distribution for the different fiber orientations shows that the maximum stress in the cylindrical composite pressure vessel is found to be minimum for (+40,-40,-40,+40) fiber orientation angle and is

equal to 36.437Mpa. The burst pressure analysis for various fiber orientations shows that the pressure vessel can bear maximum internal pressure of 185.497Mpa at (+40,-40,-40,+40) fiber orientation angle. Thus, it can be concluded from the analysis that (+40,-40,-40 and +40), fiber orientation angle is the optimum angle for the safe working of the pressure vessel. The GFRP pressure vessel if designed at (+40,-40,-40 and +40), fiber orientation angle, will have safe working conditions which can withstand maximum internal pressure.

Future Scope: As the present analysis is for cylindrical pressure vessel, it can be applied for different configurations like Spherical, Rectangular, etc. As the present work is for static analysis, we can go for dynamical analysis also. Work for the design of composite pressure vessels subjected to external pressure can be taken up. The present work can be extended to include other types of enclosures like flat and conical ends and also design of openings, supports, etc.

REFERENCES

- [1] Adali, S., Verijenko, V. E. et al. Optimization of multilayered composite pressure vessels using exact elasticity solution, *Composites for the Pressure Vessels Industry, PVP-V302, ASME*, 203-312. (1995)
- [2] Babu, M., S., Srikanth, G. & Biswas, S. *Composite Fabrication by Filament Winding - An Insight*. Retrived December 4, 2006
- [3] Chang, R. R. Experimental and Theoretical Analyses of First-Ply Failure of Laminated, Composite Pressure Vessels, *Composite Structures*, 49, 237-243. (2000)
- [4] Cohen, D., Mantell, S. C. & Zhao, L. The Effect of Fiber Volume Fraction on Filament Wound Composite Pressure Vessel Strength, *Composites: Part B*, 32, 413-429. (2001)
- [5] Crawford R. J. *Plastics Engineering* (3rd ed.). Oxford: ButterworthHeinemann (1998)
- [6] Hwang, T. K., Hong, C. S., & Kim, C. G. Size Effect on the Fiber Strength of Composite Pressure Vessels, *Composite Structures*, 59, 489-498. (2003)
- [7] Jones, R. M. *Mechanics of Composite Material* (2nd ed.). Philadelphia: Taylor & Francis. (1998)
- [8] Kabir, M. Z. Finite Element Analysis of Composite Pressure Vessels with a Load Sharing Metallic Liner, *Composite Structures*, 49, 247-255. (2000)
- [9] Lekhnitskii, S. G. *Theory of Elasticity of an Anisotropic Body*, Mir Publishers, Moscow. (1981)
- [10] Liang, C. C., Chen, H.W., Wang, C.H. Optimum Design of Dome Contour for Filament-Wound Composite Pressure Vessels Based on a Shape Factor, *Composite Structures*, 58, 469-482. (2002)
- [11] Mackerle, J. Finite Elements in the Analysis of Pressure Vessels and Piping, an Addendum: a Bibliography (1998-2001), *International Journal of Pressure Vessels and Piping*, 79, 1-26. (2002)
- [12] Mazumdar, S. K. *Composite Manufacturing: Materials, Product, and Process Engineering*. London: Crc Press. (2001)
- [13] Mirza, S., Bryan, A., Noori, M. Fiber-Reinforced Composite Cylindrical Vessel with Lugs, *Composite Structures*, 53, 143-151. (2001)
- [14] Ochoa, O. O. & Reddy, J. N. *Finite Element Analysis of Composite Laminates*. Netherland: Kluwer Academic Publishers. (1992)
- [15] Parnas, L. & Katurci, N. Design of Fiber-Reinforced Composite Pressure Vessels under Various Loading Conditions, *Composite Structures*, 58, 83-95. (2002)
- [16] Rao, V. V. S. & Sinha, P. K. Dynamic Response of Multidirectional Composites in Hygrothermal Environments, *Composite Structures*, 64, 329-338. (2004)